Infrared-absorption spectrum of an incommensurate charge-density wave: Potassium and sodium

F. E. Fragachán and A. W. Overhauser
Department of Physics, Purdue University, West Lafayette, Indiana 47907
(Received 7 May 1984)

New optical-absorption edges of a metal having a charge-density-wave ground state arise from transitions across charge-density-wave energy gaps. If the charge-density-wave wave vector $\mathbf{Q}$ is incommensurate with the reciprocal-lattice vector $\mathbf{G}$, three families of higher-order gaps in $E(\mathbf{k})$ arise: "minigaps," characterized by wave vectors $(n+1)\mathbf{Q}-n\mathbf{G}$; "heterodyne gaps," with periodicities $n(\mathbf{G}-\mathbf{Q})$; and "second-zone minigaps," with periodicities $(n+1)\mathbf{G}-n\mathbf{Q}$. The energy-gap surfaces of the first two families truncate the Fermi surface and lead to additional absorption edges in the far-infrared region. The absorption peaks associated with the first three minigaps are calculated for K and Na, and are found to be an order of magnitude larger than both the interband absorption and the main charge-density-wave peak. However, they are much smaller than the room-temperature Drude absorption. Consequently, a search for far-infrared edges must be carried out at low temperature, and in samples for which the orientation of $\mathbf{Q}$ allows observation of the Mayer—El Naby anomaly.

I. INTRODUCTION

The optical properties of the alkali metals have been studied extensively during recent years. Early measurements made by Duncan and Duncan,[1] and by Ives and Briggs,[2,3] have been analyzed in terms of the nearly-free-electron theory by Butcher,[4] Wilson,[5] and Cohen.[6] Measurements extending into the infrared have been reported by Hodgson,[7,8] Mayer and co-workers,[9,10] Althoff and Hertz[11] (far infrared), and more recently by Smith,[12] Palmer and Schnatterly,[13] and by Hietel and Mayer.[14]

This work aims to explain the nature of some observed anomalies and to predict new optical-absorption edges, in the far infrared. Our work assumes a charge-density-wave (CDW) ground state and is based on the recent improved understanding of the electronic band structure of such simple metals.[15]

In this section, we review the current, rather confused, status of the optical properties of the alkali metals. In Sec. II we present the method employed to determine the absorption coefficient, and in Sec. III we report the results obtained for sodium and potassium.

The interband optical-absorption threshold for potassium is 1.3 eV, in agreement with the theory of Butcher,[4] and the absorption intensity is weak. In 1963, Mayer and El Naby[9] discovered a rather intense optical absorption with a threshold of $\simeq 0.6$ eV, well below the normal interband threshold, in the near-infrared reflection spectrum of potassium; see Fig. 1. Most attempts to explain this anomalous absorption failed. Only one model,[16] which assumes that potassium has a CDW ground state, has given a quantitative explanation;[17] see Fig. 1 and notice the excellent agreement, based on vertical transitions across the CDW energy gap 2α created by the CDW potential. See Fig. 2. The CDW potential is

$$V_{\mathrm{CDW}}(\mathbf{r})=2\alpha\cos(\mathbf{Q}\cdot\mathbf{r})\ . \tag{1}$$

$\mathbf{Q}$ is the CDW wave vector, which in general is incommensurate with the lattice. As a consequence, a new optical-absorption mechanism, which the standard (Butcher) theory cannot account for, will arise having a threshold $\hbar\omega=2\alpha$. The theoretical absorption coefficient $(2n\kappa/\lambda)$ caused by these transitions is given by[17]

$$\frac{2n\kappa}{\lambda}=\frac{(2\alpha)^2e^2Q}{4\pi\hbar cW^2}\left[\frac{W-2\alpha}{W+2\alpha}\right]^{1/2}\left[1-\frac{W+2\alpha}{2\mu Q}\right]\cos^2\theta\ , \tag{2}$$

where W is the transition energy, n and κ are the optical constants, λ is the vacuum wavelength, $\mu\equiv\hbar^2Q/2m$, and θ represents the angle between $\mathbf{Q}$ and the photon polarization vector $\hat{\mathbf{e}}$. Therefore, the CDW optical absorption is

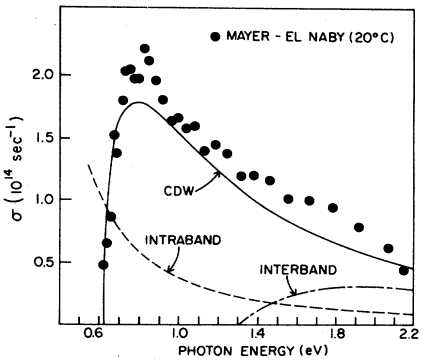

FIG. 1. Anomalous optical-absorption spectrum of potassium. The intraband conductivity (dashed curve) has been subtracted from the experimental data before being plotted. The solid curve shows the theoretical absorption introduced by a CDW structure. A normal metal would exhibit only the interband absorption with a threshold, as shown, at 1.3 eV. The anomaly is independent of temperature between 80 K and the melting point.

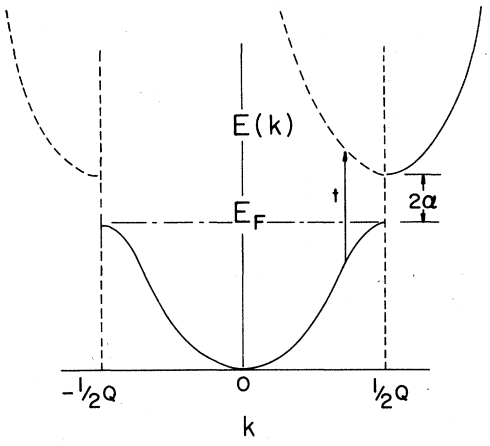

FIG. 2. Schematic behavior of $E(\mathbf{k})$, for $\mathbf{k}$ parallel to $\mathbf{Q}$, when a CDW potential, Eq. (1), is present. Optical transitions responsible for the Mayer—El Naby anomaly are indicated by the arrow "t"; the threshold is 2α (if $V_{\text{lat}}=0$).

uniaxial. This is crucial to an explanation of why the Mayer—El Naby anomaly is not seen in measurements on evaporated films. When soft metals are evaporated on amorphous substrates (e.g., glass), the crystal grains have a preferred texture. The close-packed planes of the lattice lie parallel to the surface.[18] For potassium, the normal to a glass-metal interface will be a (110) direction which, in fact, is very near to the preferred $\mathbf{Q}$ direction.[19] When light reflects from a metal surface the polarization vector (inside the metal) is parallel to the surface. As a result, $\mathbf{Q}$ is nearly perpendicular to $\hat{\epsilon}$ ($\theta=\pi/2$), and the anomalous optical absorption *cannot* occur. At bulk-metal—vacuum surfaces, the Mayer—El Naby anomaly has been reproduced by Hietel[10,20] and by Harms.[21] The intensity of the CDW absorption is (approximately) independent of temperature between 80 K and temperatures above the melting point, where the anomaly persists.[9,20]

Fäldt and Walldén[22] have suggested that the Mayer—El Naby anomaly is due to particles produced as a result of water vapor adsorption. They studied the optical properties of K films, prepared by evaporation onto a liquid-nitrogen-cooled substrate. In the photon energy range 0.6—4.0 eV they found optical anomalies after exposure of the sample to water vapor. However, they never found an anomaly with a 0.6 eV threshold. Furthermore, all new optical peaks disappeared above 110 K, unlike the Mayer—El Naby anomaly which persists even into the liquid state. Taut[23] has followed the misinterpretation of Fäldt and Walldén[22] by claiming that surface states caused by KOH are involved in the Mayer—El Naby anomaly. The absorption peaks observed by Fäldt and Walldén, which have no similarity with Harms's absorption peaks[21] (see Fig. 3), allow one to conclude that Harms's experiment actually reproduces, in a controlled way, the Mayer—El Naby anomaly. The mechanism suggested by Taut[23] requires that the optical polarization vector $\hat{\epsilon}$ have a component perpendicular to the surface, which would occur for a rough surface. Possibly the absorption peaks observed by Fäldt and Walldén involve

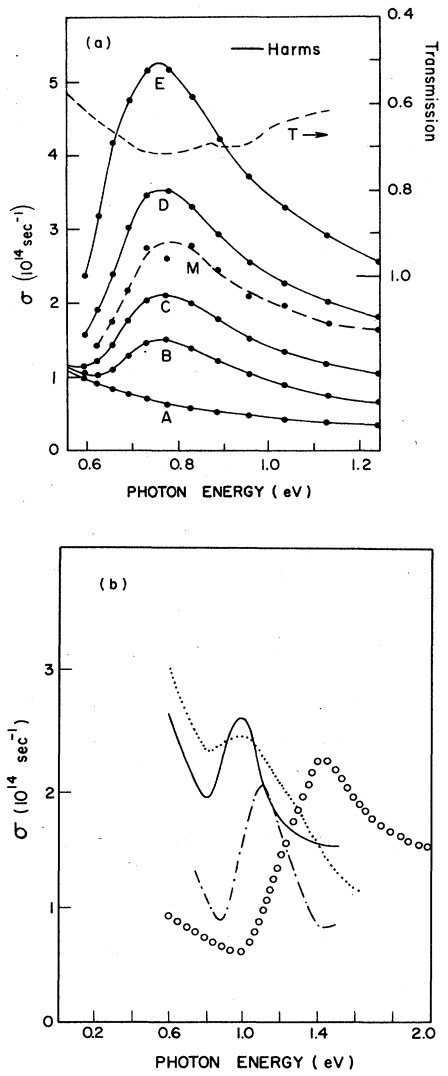

FIG. 3. Comparison between (a) Harms's experiment, Refs. 19 and 21, and (b) Faldt and Walldén, Ref. 22. (a) Curve A is the optical conductivity (absorption) of a fresh bulk-potassium-vacuum interface. Curves B, C, D, and E were obtained on the same specimen after successive exposure to trace amounts of H_2O. The dashed curve M is one obtained by Mayer and El Naby, Ref. 9. The dashed curve T is an inverted plot of the optical transmission through 0.01 cm of KOH. All data were taken at room temperature. (b) The optical conductivity of an evaporated film of potassium after exposure to trace amounts of H_2O. The substrate was at 78 K. The absorption peaks caused by the exposure occur at various photon energies in different experimental runs. All structure disappeared above 110 K.

surface states since they disappeared at the same temperature as the surface plasmon peak (which also requires a rough surface).

The CDW anomaly in Na has a 1.2-eV threshold.[14] Not only does it persist into the liquid metal (as in K), where the metal-vacuum interface is smooth, but is largest there. The influence of slight amounts of water vapor on the intensity of the Mayer—El Naby peak, but not on its

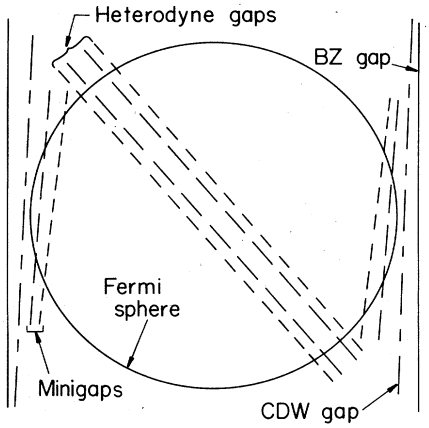

FIG. 4. Free-electron Fermi sphere and various energy gaps caused by a CDW. Only two (of the 12) Brillouin-zone gaps, solid vertical lines, are shown.

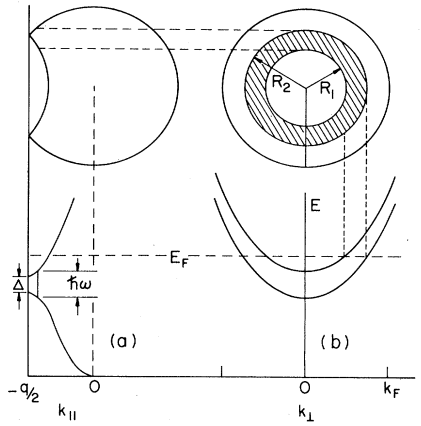

FIG. 5. Portions of the Fermi sphere responsible for optical absorption caused by a minigap of magnitude Δ. (a) is a side view and (b) is a front view (along a line parallel to **q**). Relevants plots of $E(\mathbf{k})$ are shown.

spectral shape or location (unlike the various peaks of Fäldt and Walldén; see Fig. 3), can be explained by the influence of KOH layers on the crystallographic orientation at the metal surface,[19] which alters θ in Eq. (2).

The existence of this new absorption mechanism indicates that one must consider a Schrödinger equation having a potential

$$V(\mathbf{r})=2\alpha\cos(\mathbf{Q}\cdot\mathbf{r})+V_{\text{lat}}(\mathbf{r})\ , \tag{3}$$

i.e., two incommensurate periodic potentials: a CDW potential and a lattice pseudopotential:

$$V_{\text{lat}}=2\beta\cos(\mathbf{G}\cdot\mathbf{r})\ . \tag{4}$$

$|\mathbf{Q}|\simeq 1.36-1.38(2\pi/a)$ and $|\mathbf{G}|=1.414(2\pi/a)$; a is the lattice constant and $|\mathbf{G}|$ is the magnitude of the (110) reciprocal-lattice vector. Solution of the Schrödinger equation having Eq. (3) for the potential leads to three main families of energy gaps which we name as follows (in accordance with their wave-vector periodicities, **q**).

(a) For minigaps:

$$\mathbf{q}=(n+1)\mathbf{Q}-n\mathbf{G}\ . \tag{5}$$

(b) For heterodyne gaps:

$$\mathbf{q}=n(\mathbf{G}-\mathbf{Q})\ . \tag{6}$$

(c) For second-zone minigaps:

$$\mathbf{q}=(n+1)\mathbf{G}-n\mathbf{Q}\ . \tag{7}$$

There remain, of course, the energy gaps at the Brillouin-zone faces perpendicular to **G**, and the CDW gaps shown in Fig. 2. For each type, $n=1,2,3,\ldots$. Only the minigaps and the heterodyne gaps truncate the Fermi sphere, as shown in Fig. 4.

II. MINIGAP ABSORPTION

We shall now calculate the optical-absorption coefficient associated with the first three minigaps as if each in turn were created by a potential of the form

$$V(\mathbf{r})=\Delta\cos(\mathbf{q}\cdot\mathbf{r}),\quad |\mathbf{q}|<2k_F\ , \tag{8}$$

see Fig. 5. Δ is the minigap and **q** is the minigap wave vector. It turns out that independent treatment is not a good approximation for the heterodyne gaps and, therefore, we have left them for a future analysis.

In light of Fig. 5(b), we can see qualitatively that the optical absorption is caused by vertical transitions from the lower to the upper band, and that the threshold energy is $\hbar\omega=\Delta$. Note that both bands are occupied at $k_\perp=0$ (near the gap) so no absorption can occur there. However, as we move parallel to the energy-gap plane the two branches of $E(\mathbf{k})$ are parallel and separated by Δ. Hence, absorption can occur on the portion of the plane shown shaded in Fig. 5(b). For simplicity we neglect any deformation of the Fermi surface caused by the potential in Eq. (8). (It can easily be included, and we will comment later on what the effect would be.)

The wave function $\Phi_{\mathbf{k}'}$ of an electron, in the neighborhood of the gap at A, Fig. 6, below the gap, is

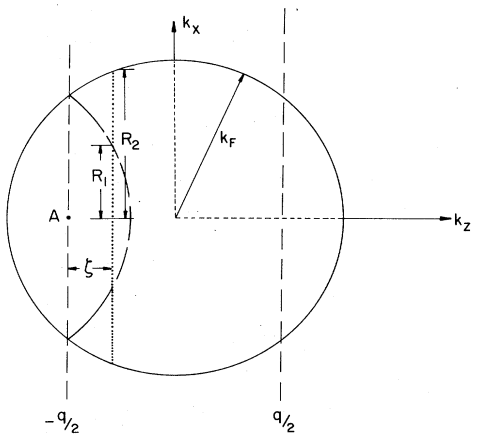

FIG. 6. Schematic view of the Fermi sphere with parameters employed in the text to derive the minigap absorption from states along the dotted vertical line.

$$\Phi_{\mathbf{k}'}=\sin\gamma e^{i\mathbf{k}'\cdot\mathbf{r}}-\cos\gamma e^{i(\mathbf{k}'+\mathbf{q})\cdot\mathbf{r}} . \quad (9)$$

The corresponding state above the gap, which is connected with $\Phi_{\mathbf{k}'}$, in an absorption event, is,

$$\Phi_{\mathbf{k}}=\cos\gamma e^{i\mathbf{k}\cdot\mathbf{r}}+\sin\gamma e^{i(\mathbf{k}+\mathbf{q})\cdot\mathbf{r}} . \quad (10)$$

The coefficients obey the relation[17]

$$\sin 2\gamma=\frac{\Delta}{E_+-E_-}\equiv\frac{\Delta}{W} , \quad (11)$$

with

$$E_\pm=\epsilon_k+\mu\zeta\pm\left[\mu^2\zeta^2+\frac{\Delta^2}{4}\right]^{1/2} , \quad (12)$$

where $\epsilon_k=\hbar^2k^2/2m$, $\mu\equiv\hbar^2q/2m$, ζ is the perpendicular distance in $\mathbf{k}$ space from the gap at A (Fig. 6), and $W\equiv E_+-E_-$ is the vertical transition energy.

The macroscopic photon field in a metal can be described by a vector potential

$$\mathbf{A}(z)=\hat{\boldsymbol{\epsilon}}e^{-\kappa\omega z/c}\cos\left[n\frac{\omega}{c}z-\omega t\right] , \quad (13)$$

where $\hat{\boldsymbol{\epsilon}}$ is the unit polarization vector of the electric field and n and κ are the optical constants. The interaction Hamiltonian of an electron with this potential is

$$H'=\frac{e}{mc}\mathbf{A}\cdot\mathbf{p} . \quad (14)$$

The strategy of the calculation is to calculate the flow of energy at $z=0^+$ and equate it to the transition rate times $\hbar\omega$ caused by the perturbation H'. The flow of energy at $z=0^+$ is, from Poynting's vector,

$$P=\frac{c}{4\pi}\langle\,|\,\mathbf{E}\times\mathbf{H}\,|\,\rangle=\frac{n\omega^2}{8\pi c} , \quad (15)$$

where the $\langle\ \rangle$ indicates time averaging. The last equality follows from Eq. (13), with $\hat{\boldsymbol{\epsilon}}$ along $\hat{\mathbf{x}}$. On the other hand, the transition rate caused by the perturbation is, with $W\equiv\hbar\omega$,

$$\frac{P}{W}=4\sum_{\mathbf{k}',\mathbf{k}}\left[\frac{2\pi}{\hbar}\right]\langle\,|\,V_{\mathbf{k}',\mathbf{k}}\,|^2\rangle\delta(E_{\mathbf{k}}-E_{\mathbf{k}'}-\hbar\omega) , \quad (16)$$

where the factor 4 takes account of the spin degeneracy and the two gaps at opposite sides of the Fermi surface. From Eqs. (9), (10), (13), and (14) one finds (considering only the contribution from absorption)

$$\langle\,|\,V_{\mathbf{k}',\mathbf{k}}\,|^2\rangle=\left[\frac{\hbar e\hat{\boldsymbol{\epsilon}}\cdot\mathbf{q}\sin\gamma\cos\gamma}{2mc}\right]^2\times\left[\left[k_z'-k_z+n\frac{\omega}{c}\right]^2+\left[\kappa\frac{\omega}{c}\right]^2\right]^{-1} . \quad (17)$$

The $\mathbf{k}$ components transverse to $\mathbf{z}$ are conserved. Changing the k sum in Eq. (16) to an integral (and using properties of the δ function) we obtain

$$\frac{P}{W}=4\left[\frac{2\pi}{\hbar}\right]\sum_{k_z'}\frac{1}{(2\pi)^3}\int\,|\,V_{k_\omega',k_z}\,|^2\frac{dS}{|\,\nabla_{\mathbf{k}}(E_{\mathbf{k}}-E_{\mathbf{k}'})\,|} , \quad (18)$$

where the integration is over a surface of constant transition energy, $E_{\mathbf{k}}-E_{\mathbf{k}'}$, and for which $\mathbf{k}$ is occupied and $\mathbf{k}'$ is empty. The matrix element will not change as $\mathbf{k}$ is swept over this surface, so we take it outside the integral:

$$\frac{P}{W}=4\left[\frac{2\pi}{\hbar}\right]\sum_{k_z'}\,|\,V_{k_z',k_z}\,|^2\frac{1}{(2\pi)^3}\int\frac{dS}{|\,\nabla_{\mathbf{k}}(E_{\mathbf{k}}-E_{\mathbf{k}'})\,|} . \quad (19)$$

The joint density of states (dN/dW) for unit volume is

$$\frac{dN}{dW}=\frac{1}{(2\pi)^3}\int\frac{dS}{|\,\nabla_{\mathbf{k}}(E_{\mathbf{k}}-E_{\mathbf{k}'})\,|} . \quad (20)$$

Hence,

$$\frac{P}{W}=4\left[\frac{2\pi}{\hbar}\right]\frac{dN}{dW}\sum_{k_z'}\,|\,V_{k_\omega',k_z}\,|^2 . \quad (21)$$

We evaluate the summation over k_z' by converting it to an integral:

$$\frac{P}{W}=4\left[\frac{2\pi}{\hbar}\right]\frac{dN}{dW}\frac{1}{2\pi}\int_{-\infty}^{\infty}\,|\,V_{k_\omega',k_z}\,|^2dk_z' . \quad (22)$$

Since Eq. (17) is a Lorentzian, the integration is trivial. We obtain

$$P=\frac{4\pi c}{\kappa}\frac{dN}{dW}\left[\frac{\hbar eq\Delta\cos\phi}{4mcW}\right]^2 , \quad (23)$$

with ϕ being the angle between $\hat{\boldsymbol{\epsilon}}$ and $\mathbf{q}$. [We have used Eq. (11) to eliminate $\sin\gamma$ and $\cos\gamma$.] From Eqs. (15) and (23) we find the theoretical absorption coefficient:

$$\frac{2n\kappa}{\lambda}=\frac{2\pi\hbar^3}{cW^3}\left[\frac{e}{m}q\Delta\cos\phi\right]^2\frac{dN}{dW} . \quad (24)$$

The density of states will be determined below.

III. RESULTS FOR K and Na

In order to calculate the optical-absorption spectrum caused by transitions across the minigaps we need to know their sizes.[15] This requires knowledge of the CDW gap, 2α, and the (110) pseudopotential, β. Unfortunately, the value of β is still an unanswered question. Estimates vary by up to a factor of 3. For example, analyses[24,25] of Fermi-surface anisotropy (from de Haas–van Alphen data) which assume local pseudopotentials lead to values at the higher limit. Much lower values are obtained when nonlocal pseudopotentials[26] are employed. The ranges for the magnitudes of β are

$$\beta_{\mathrm{K}}=0.07\text{–}0.2\ \mathrm{eV} , \quad (25a)$$

$$\beta_{\mathrm{Na}}=0.12\text{–}0.23\ \mathrm{eV} . \quad (25b)$$

The lower values create a problem with regard to the intensity of the ordinary (Wilson-Butcher) interband optical absorption, since this is proportional to β^2. Serious discrepancy with experiment results unless enhancement of the matrix element by the collective effects of exchange and correlation are included.[27]

TABLE I. Minigaps and heterodyne gaps obtained for several values of **Q** for K and Na. All gaps are in meV. $|\mathbf{Q}|$ is in $2\pi/a$ units. ($\beta \equiv |V_{110}|$.)

$\lvert\mathbf{Q}\rvert$	First minigap	Second minigap	Third minigap	First heterodyne	Second heterodyne	Third heterodyne
			Potassium, $\beta=0.20$ eV			
1.36	97	27	3	27	9	1
1.37	106	43	9	28	12	2
1.38	107	62	25	28	16	5
			Potassium, $\beta=0.07$ eV			
1.36	33	5.9	0.10	8.4	0.94	0.03
1.37	38	7.1	0.26	8.4	1.40	0.06
1.38	44	11	0.91	8.4	2.3	0.19
			Sodium, $\beta=0.23$ eV			
1.37	138	57	11	38	14	2
1.38	135	79	31	38	20	5
1.39	116	87	63	37	25	13
			Sodium, $\beta=0.12$ eV			
1.37	75	18	1.5	18	4	0.25
1.38	80	29	4.5	18	6.1	0.71
1.39	78	46	17	17	9.2	2.6

The CDW potential 2α can be estimated from the threshold of the Mayer–El Naby optical anomaly.[17] As mentioned in the Introduction, the observed threshold is 0.62 and 1.2 eV for K and Na, respectively.

As shown in Fig. 4, there is a small angle θ between **Q** and **G**.[15,28,29] This small tilt leads to several problems in calculating the sizes of the various minigaps. The first is that the gaps no longer lie on planes perpendicular to **q** (and which pass through $\pm\mathbf{q}/2$, see Fig. 6). Instead the gaps define curved surfaces in **k** space which are close to the planes described. To find such a surface, consider a coordinate system with $\hat{\mathbf{z}}$ parallel to **q** and $\hat{\mathbf{x}}$ in the plane containing **Q**, **G**, and **q**. For a fixed k_x, plot the optical transition energy versus k_z. The minimum transition energy is the value of the minigap (for that k_x), and the location k_z of the energy-gap surface is at the value of k_z having that minimum. We found that the gaps vary quadratically with k_x, with minima near $k_x=0$. The values obtained for the first three minigaps are given in Table I where, for completeness, we have also included the heterodyne gaps.

In order to determine the joint density of states, allow (as a first approximation) **Q** to be parallel to **G**. For this situation, the joint density of states is obtained by calculating the shaded area in Fig. 5(b) for a small disc of width $d\zeta$ at a distance ζ from point A (see Fig. 6), i.e. (R_1 and R_2 are found by simple geometry from Fig. 6),

$$\frac{dN}{dW}=\frac{1}{(2\pi)^3}\pi(R_2^2-R_1^2)\frac{d\zeta}{dW}\ , \tag{26}$$

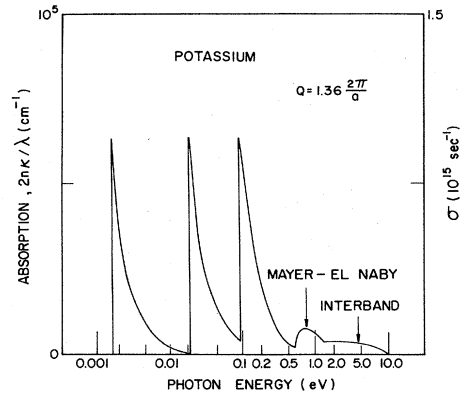

FIG. 7. Optical-absorption spectrum of potassium for $|\mathbf{Q}|=1.36(2\pi/a)$ and **Q** parallel to **G**. ($2n\kappa/\lambda=2\sigma/c$.) The zone boundary energy gap 2β has been taken to be 0.4 eV, and the Drude absorption has been ignored. For room temperature the Drude absorption at 0.1 eV would be 4 times larger than the peak from the minigap at 0.1 eV. For $\beta=0.07$ eV the first minigap threshold occurs at 0.04 eV (instead of 0.1).

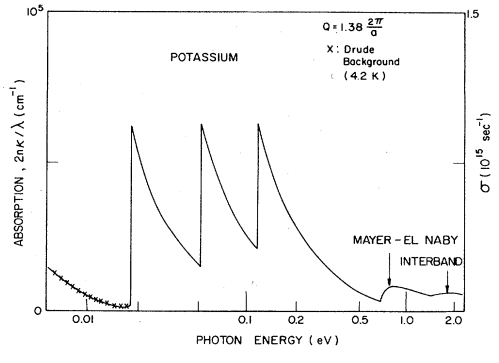

FIG. 8. Drude background (X) at 4.2 K and the total absorption coefficient (or conductivity) of potassium for $|\mathbf{Q}|=1.38(2\pi/a)$ and **Q** parallel to **G**. The zone boundary energy gap was assumed to be $2\beta=0.4$ eV.

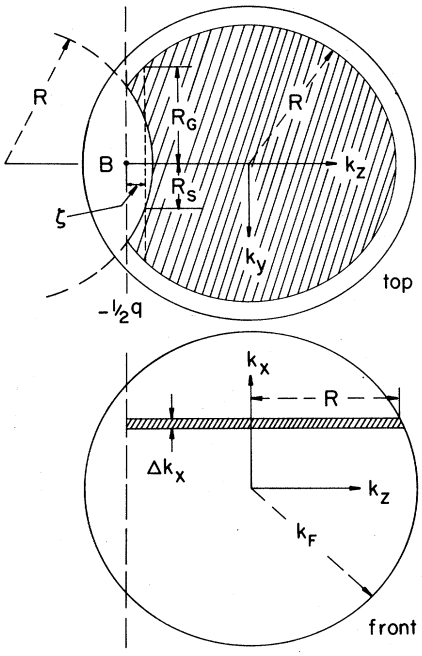

FIG. 9. Projections of the Fermi sphere used to calculate the absorption when **Q** is not parallel to **G**. Each disc (of thickness Δk_x, shown in the front view) has a slightly different energy gap at $k_z=-q/2$. Only the shaded region of the top view has unoccupied final states.

if $0\leq\zeta<(k_F-q/2)$, with $2k_F=1.24(2\pi/a)$; for $\zeta\geq(k_F-q/2)$, $R_1=0$. Therefore (for **Q** parallel to **G**) we obtain

$$\frac{2n\kappa}{\lambda}=\frac{e^2\Delta^2 q}{2\pi c\hbar W^2}\cos^2\phi \quad \text{if } 0\leq\zeta<\left[k_F-\frac{q}{2}\right] \tag{27}$$

and

$$\frac{2n\kappa}{\lambda}=\frac{e^2\Delta^2 q}{2\pi c\hbar W^2}\frac{(\hbar^2R_2^2/2m)}{(W^2-\Delta^2)^{1/2}}\cos^2\phi \quad \text{if } \zeta\geq\left[k_F-\frac{q}{2}\right]. \tag{28}$$

This absorption spectrum is shown in Figs. 7 and 8 for K. We have included the first three minigaps and have used alternative values for **Q**. We have taken $\langle\cos^2\phi\rangle=\frac{1}{3}$. In Fig. 8 we have included the contribution from intraband transitions (Drude background) at 4.2 K, assuming a sample with a residual resistivity ratio of $\simeq$6000. At room temperature the Drude background is too high for these new absorption edges to be observed. This is the reason why any search for such new edges must be done at low temperatures.

Finally we turn to the evaluation of the joint density of states when the small tilt between **Q** and **G** is considered. In this situation, because of the variation of the gap with k_x, we fix k_x, as shown in Fig. 9, and consider the k_y-k_z plane (Δk_x thick) corresponding to that fixed k_x. The joint density of states in a small "disc" of width $d\zeta$, a distance ζ from point B, Fig. 9, is given by

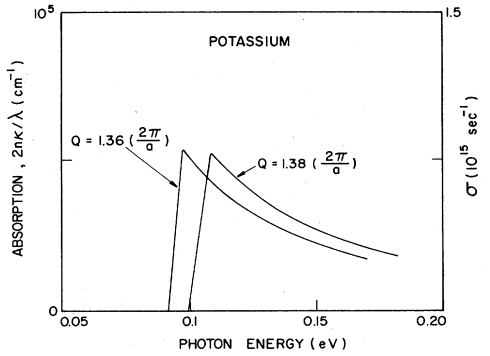

FIG. 10. Optical-absorption spectrum of the first minigap of potassium showing the gradual rise at threshold caused by the small angle between **Q** and **G**. The zone boundary energy gap 2β was assumed to be 0.4 eV. The threshold is reduced to $\simeq$0.04 eV if $2\beta=0.14$ eV.

$$\frac{dN}{dW}=\frac{1}{(2\pi)^3}(2R_G-2R_S)\Delta k_x\frac{d\zeta}{dW}. \tag{29}$$

Therefore,

$$\frac{2n\kappa}{\lambda}=\sum_{k_x}\frac{2\pi\hbar^3}{cW^3}\left[\frac{e}{m}q\Delta\cos\phi\right]^2\frac{dN}{dW}. \tag{30}$$

The important dependence on $\cos^2\phi$ should be noted. It implies that the minigap absorption is also uniaxial. The spectrum is obtained by numerical evaluation of the sum over k_x. Examples for the first minigap in K are shown in Fig. 10 for several values of $|\mathbf{Q}|$. The major difference from the results obtained in Figs. 7 and 8, with **Q** parallel to **G**, is that the sudden rise in absorption at threshold is less abrupt. Had we included the slight distortion of the Fermi surface near the energy gaps, the rise in absorption at threshold would be somewhat steeper.

The absorption profiles of all the minigaps are very much alike. The peaks are about an order of magnitude larger than the interband absorption or the main CDW anomaly. We emphasize once again that the threshold values given in Table I are subject to uncertainty because the pseudopotentials of the periodic lattice are not known from a direct experiment.

IV. CONCLUSIONS

We have found that new optical-absorption edges in the far-infrared spectrum of a metal having a CDW ground state arise from transitions across the minigaps. The absorption peaks associated with the first three minigaps have been calculated for K and Na and found to be about an order of magnitude larger than both the interband and the main CDW peak. However, they are much smaller than the room-temperature Drude background. Therefore

any search for such edges must be carried out at low temperatures, where the Drude background is significantly reduced, and in samples for which the orientation of **Q** allows the observation of the Mayer—El Naby anomaly. The minigap absorption, as well as the main CDW absorption, is *uniaxial.*

ACKNOWLEDGMENTS

This research was supported by the National Science Foundation and for one of us (F.E.F.) by the Energy and Mine Department, Venezuela.

[1]R. W. Duncan and R. C. Duncan, Phys. Rev. **1**, 294 (1913).
[2]H. E. Ives and H. B. Briggs, J. Opt. Soc. Am. **26**, 238 (1936).
[3]H. E. Ives and H. B. Briggs, J. Opt. Soc. Am. **27**, 181 (1937).
[4]P. N. Butcher, Proc. Phys. Soc. London, Sect. A **64**, 765 (1951).
[5]A. H. Wilson, *The Theory of Metals* (Cambridge University Press, Cambridge, 1958).
[6]M. H. Cohen, Philos. Mag. **3**, 762 (1958).
[7]J. N. Hodgson, J. Phys. Chem. Solids **24**, 1213 (1963).
[8]J. N. Hodgson, Phys. Lett. **7**, 300 (1963).
[9]H. Mayer and M. H. El Naby, Z. Phys. **174**, 269 (1963); **174**, 280 (1963); **174**, 289 (1963).
[10]H. Mayer and B. Hietel, in *Proceedings of the International Colloquium on Optical Properties and Electronic Structure of Metals and Alloys, Paris, 1965,* edited by F. Abeles (North-Holland, Amsterdam, 1966), p. 47.
[11]R. Althoff and J. H. Hertz, Infrared Phys. **7**, 11 (1967).
[12]N. V. Smith, Phys. Rev. **183**, 634 (1969).
[13]R. E. Palmer and S. E. Schnatterly, Phys. Rev. B **4**, 2329 (1971).
[14]B. Hietel and H. Mayer, Z. Phys. **264**, 21 (1973).
[15]F. E. Fragachán and A. W. Overhauser, Phys. Rev. B **29**, 2912 (1984).
[16]A. W. Overhauser, Phys. Rev. Lett. **4**, 462 (1960); Phys. Rev. **128**, 1437 (1962); **167**, 691 (1968); Adv. Phys. **27**, 343 (1978).
[17]A. W. Overhauser, Phys. Rev. Lett. **13**, 190 (1964).
[18]R. C. Jaklevic and J. Lambe, Phys. Rev. B **12**, 4146 (1975).
[19]A. W. Overhauser and N. R. Butler, Phys. Rev. B **14**, 3371 (1976).
[20]B. Hietel (private communication).
[21]P. Harms, dissertation, Technischen Universitat Clausthal, 1972 (unpublished); his data are reproduced in Ref. 19.
[22]Å. Fäldt and L. Walldén, J. Phys. C **13**, 6429 (1980).
[23]M. Taut, J. Phys. F **12**, 2019 (1982).
[24]A. W. Overhauser (unpublished).
[25]N. Ashcroft, Phys. Rev. **140**, A935 (1965).
[26]M. J. G. Lee, in *Computational Methods in Band Theory,* edited by P. M. Marcus, J. F. Janak, and A. R. Williams (Plenum, New York, 1971).
[27]A. W. Overhauser, Phys. Rev. **156**, 844 (1967).
[28]G. F. Giuliani and A. W. Overhauser, Phys. Rev. B **20**, 1328 (1979).
[29]For $|\mathbf{Q}| \simeq 1.36 \rightarrow 1.38(2\pi/a)$, $\theta \simeq 2.6° \rightarrow 1.6°$. See Ref. 15.